

Received Date : 11-Oct-2014

Revised Date : 18-Jan-2015

Accepted Date : 18-Feb-2015

Article type : Research Article

Combined Molecular Docking, 3D-QSAR, and Pharmacophore Model: Design of Novel Tubulin Polymerization Inhibitors by Binding to Colchicine- binding Site

Dong-Dong Li^{a,}, Ya-Juan Qin^{b,†}, Xin Zhang^b, Yong Yin^b, Hai-Liang Zhu^{b*}*

^a College of Chemical Engineering, Nanjing Forestry University, Nanjing, 210073, P. R. China.

^b State Key Laboratory of Pharmaceutical Biotechnology, School of Life Sciences, Nanjing University, Nanjing, 210093, P. R. China.

Corresponding Author

* Dong-Dong Li, Tel.: +86 025 85427962; E-mail: lidon@njfu.edu.cn. Hai-Liang Zhu, Tel.: +86-25-8359 2572; Fax: +86 025 83592672; E-mail address: zhuhl@nju.edu.cn. Lin-Guo Zhao, E-mail: lgzhao@njfu.edu.cn.

This article has been accepted for publication and undergone full peer review but has not been through the copyediting, typesetting, pagination and proofreading process which may lead to differences between this version and the Version of Record. Please cite this article as an 'Accepted Article', doi: 10.1111/cbdd.12545

This article is protected by copyright. All rights reserved.

Author Contributions

‡These authors contributed equally.

ABSTRACT

Interference with dynamic equilibrium of microtubule-tubulin has proven to be a useful tactics in the clinic. Based on investigation into the structure–activity relationship (SAR) studies of tubulin polymerization Inhibitors obtained from several worldwide groups, we attempted to design 691 compounds covering several main heterocyclic scaffolds as novel colchicine site inhibitors (CSIs). Evaluated by a series of combination of commonly used computer methods such as molecular docking, 3D-QSAR, and pharmacophore model, we can obtain the ultimate 16 target compounds derived from five important basic scaffolds in the field of medicinal chemistry. Among these compounds, compound **A-132** with *in silico* moderate activity was synthesized, and subsequently validated for preliminary inhibition of tubulin polymerization by immunofluorescence assay. In additional, the work of synthesis and validation of biological activity for other 15 various structure compounds will be completed in our lab. This study not only developed a hierarchical strategy to screen novel tubulin inhibitors effectively, but also widened the spectrum of chemical structures of canonical CSIs.

KEYWORDS: Microtubules; Antitumor agents; Colchicine-binding site; 3D-QSAR; Pharmacophore.

INTRODUCTION

Targeting the process of microtubule dynamics contributes much for cancer therapies, due to it plays an crucial role in the maintenance of cell shape, signal transduction, and chromosome segregation during mitosis (1). So far, microtubule-targeting agents could be simply classified into microtubule stabilizer and microtubule destabilizer according to the mechanism by interfering with microtubule dynamics. Further divided, there are four major binding sites provided by the microtubule: the taxane site and the laulimalide/ peloruside A site for microtubule stabilizer, and the vinca site and the colchicine site for microtubule destabilizer (2).

The motivations for developing colchicine site inhibitors (CSIs) can be concluded as follows. Firstly, by comparison of the two successful antitumor drugs taxanes and vinca alkaloids, the first CSI colchicine (Figure 1), while inhibiting cancer cell proliferation potently, has limited its applications in clinical trials as antitumor agent due to its narrow therapeutic index (3). Much possibility for searching novel scaffolds into the CSI chemical space will be provided. Currently the CSI-like compound most close to the drug approved by FDA is CA-4P (Zybrestat, Figure 1), which is being developed under clinical trials as a treatment for solid tumors. Second, a large number of small molecules binding to colchicine site have been reported, which possess significant structural diversity. Meanwhile consideration in the development of CSIs as vascular disrupting agents (3) (VDA) that obviously differs from cytotoxic agents such as taxanes and vinca alkaloids, This will stimulate the exploitation of CSIs in the further step. Thirdly, molecular complexity of colchicine site inhibitors are less than that of taxol and vinca site binders, which could be in more favor of exploring the CSI chemical space efficiently (5). In addition, unsolved problems such as multiple drug resistance (MDR) and secondary toxicity induced by common cytotoxic agents in the clinical use might be circumvented by means of colchicine site agents (6, 7). Thus, there is an urgent need to design and synthesize novel tubulin inhibitors based on the colchicine site at the β -tubulin.

To date, there are dozens of CSIs (Figure 1) being evaluated under clinical investigation, and even more in preclinical studies, mainly including combretastatin analogs, indole-, quinolone- and thiophene-based compounds, chalcone compounds, and sulfonanilide compounds (3). Such structural diversity of the CSIs seems to be closely involved with the inherent flexibility of the binding site, which can be demonstrated by several tubulin protein crystal structures (PDB ID: 1SA0 (8), 1SA1 (9), 3HKC (10), 3HKE (10), 3HKD (10), 3N2K (11), and 3N2G (11)).

Based on the increased crystal structures related to the colchicine site, an increasing number of computer modeling studies of CSIs have been reported (12-14). However, that all the available crystal structures of tubulin protein complex have low resolution (3.5~4.0 Å, Table S1) leads to less success in structure-based drug discovery. The way by employing combination of 3D-QSAR, docking studies and molecular dynamics simulations actually improved accuracy of computer model (15). Additionally, there are very few reports about discovering novel tubulin inhibitors using curated design and a series of structure-based virtual screening (VS) methods. Therefore, in this manuscript, we would attempt to design novel CSIs based on the widely-used tubulin crystal complex 1SA0 as the drug target template.

In order to discover novel tubulin inhibitors, the detailed investigation of the compounds that were collected from recently published papers for structure–activity relationship (SAR), together with binding site analyses, was displayed in Chart 1. On the basis of the above results, the curated process of designed compounds was performed on the seven basic scaffolds (Figure S1). As to these compounds with structural diversity, we developed a hierarchical strategy for structure-based virtual screening (VS) by integrating different computational methods (Figure 2). Briefly, the whole procedure could be depicted in the successive five steps: (1) On the basis of the SAR analysis, designing 691 novel small molecules covering seven basic scaffolds; (2) Predicting the binding poses of ligands using the CDOCKER docking program (16); (3) Optimizing and calculating the binding energy of the docked ligand in protein binding pocket by molecular mechanics (MM) force field in combination with generalized born surface area (GB/SA) implicit solvent (17); (4) With the help of those 115 reported active tubulin inhibitors (Figure S2) extracted from recent papers, building 3D-QSAR models located in the colchicine site using the Discovery Studio suite 3.5 (18); (5) The establishment of pharmacophore modeling based on ten docked ligands with high activity in the binding site, also built by the Discovery Studio suite 3.5. In each step, the predefined filters were applied to eliminate the undesired hits, and it was expected that such hierarchical protocol can maximally reduce the false positives produced by the manual experience-based judgment, which finally led to that the top 16 novel molecules were obtained. In the next section, we would elaborate this series of processes above in detailed.

RESULTS AND DISCUSSION

Investigation into the SAR of Compounds with Various Scaffolds

As said above, many recently published good works had been selected for optimizing our strategy, particularly continuous studies from the same group. We retrieved the term “tubulin” on the *J. Med. Chem.* website, and curated sixteen important medicinal chemistry papers (19-34) carefully for analysis of the structure-activity relationship (SAR) and the binding pose of these ligands (Chart 1). From the year 2004 to 2012, Silvestri group (19-24) reported a series of colchicine site inhibitors with arylthioindole skeleton, and recently their attentions were shift to the replacement of the indole ring with thiazole (25, 26). Kremmidiotis group (27) depicted a class of tubulin polymerization inhibitors derived from the benzofuran scaffold, in which compound **95** (**BNC105**, Figure 1) had been investigated under the clinical trial. Chang group (28, 29) reported that compounds containing 5-amino-2-arylquinolines skeleton possessed the inhibitory activities towards tubulin polymerization. In recent years Li group (33,34) reported that a class of 4-Aryl-2-benzoyl-imidazoles (ABI-III) were developed as as Tubulin Polymerization Inhibitors. In addition, several kinds of CSIs with various aromatic ring system as basic skeleton (30-32) were also reported.

Due to the inherent flexibility of the binding site, colchicine-binding pocket could accommodate various structure ligands. In aim to probe the role of structural diversity of these compounds as CSIs, the molecular docking studies of these optimized compounds from the above literatures were performed based on the common tubulin protein crystal complex (PDB code: 1SA0), and subsequently the reasonable conformations of these compounds were manually selected. Referring to the obtained poses located at the binding site, we artificially divided the modification space into four small-size regions (A: the modifications of the linker; B and C: the modifications of substituents of the parent nucleus; D: the modifications of the trimethoxybenzoyl “headgroup”). While this kind of simple classification appeared to be arbitrary, it actually was in much favor of exploring the SARs of these compounds.

It is worthwhile noting that these compounds seemed to possess much of the same structural features when focusing the binding pose at the colchicine-binding site (Chart 1). Firstly, almost all the optimized compounds contained trimethoxybenzoyl moiety, which could be inserted into the same position of the active pocket. It is the prerequisite for inhibition of tubulin polymerization. Focusing on D region, the methoxy group at the *para* position

Accepted Article

can largely influence tubulin inhibitory activity (20), and a halo or a nitro group at the *ortho* position can moderately increase potency (30). Second, how to carry on the modifications of B and C region heavily depended on the structure of the parent nucleus (indol, thiophene, thiazole, or otherelse). The common electron-donating group such as hydroxy, methoxy, amino or halo substituent can be employed at this site for enhancing potency (19-21, 23, 27-30). The difference of modification on B and C area between these lead compounds was merely the various position of the parent core. Another interest point was that the B region could accommodate a large-size group, no matter hydrophobic or hydrophilic substituent (27). Besides, the alternation of the parent nucleus could circumvent tumor resistance (31). The compounds with mono-aromatic ring system (thiazole or thiophene) might possess much of variation on alternative binding pose (26, 27), thus this needed to be discussed carefully in the design process of novel CSIs. Thirdly, the SAR studies (19-24) on the linker of a series of arylthioindole compounds revealed that A region tended towards the rigid moiety, such as ketone or amide, while the methylene can be tolerated (23). However, as to compounds with mono-aromatic ring as the parent nucleus, the analysis of their binding pose displayed that the mono-aromatic ring could act as a role of the linker group (27, 33, 34).

Design CSIs based on the SAR Study and Limited Laboratory Conditions

In this section, we delineated our approach for the design of novel CSIs (Figure 3). It started with the employment of seven basic scaffolds (A-series: indol; B-series: thionaphthene; C-series: benzofuran; D-series: imidazole; E-series: parazole; F-series: benzimidazole; G-series: 1,3,4-Oxadiazole). A-, B, and C-series were the common basic scaffolds for developing tubulin inhibitors, while the rest could be regarded as new basic entities. Besides, for E- and G-series, there were a large number of works (35-40) reported in our group, which can provide the practical basis for synthesizing these two kinds of compounds in the future.

As to A-series, we retained the bromine or nitro group at the *ortho* position of trimethoxybenzoyl headgroup (D region), the bromine or methoxy group at the C-5 position of the indol ring (C region), and methoxy/ethoxycarbonyl group at position 2 of the indole nucleus (B region) on the basis of the SAR studies. Considering that the rigidity of the linker bridge (A region) and the aromatic moiety at B region would enhance oral bioavailability of compounds, we introduced the four various length of rigid linkages (Figure 3, **A-series**) for bridging the indole nucleus and trimethoxybenzoyl headgroup, and attached the 1,3,4-Oxadiazole aromatic system that was easy to be synthesized

to the C-2 position of the parent core. After carefully checking whether this kind of molecules had been reported previously, the number of the molecules belong to A-series reached up to 143. Compared B and C series to A series, the only difference focused on additional amino group that was closely related to the parent core (21). The number of B and C series was 152 and 153, respectively. For the mono-aromatic ring (D-, E-, G-series), the designed process seemed to be slightly complicated, due to docking study indicated that the binding conformation of these classes of compounds in the active pocket would vary with the modification at the different position. As to D-series, this sort of molecules can be further classified into three blocks (D1: trimethoxybenzoyl group at the C4-position and amino group at the C-2 position of the imidazole nucleus; D2: trimethoxybenzoyl group at the C4-position and amino group at the C-5 position; D3: trimethoxybenzoyl group at the C2-position), according to the grafted position of trimethoxybenzoyl and amino group on the imidazole ring. In addition, owing to the small size of the imidazole core, it was surmised that this scaffold could spin in the deep active pocket (33, 34). Thus, it was a bit difficult to differentiate the modification at B or C region clearly. This stimulated us to consider the design of compounds **132~143**, mainly due to that it was not sure at which position of these indole-pyrazole analogs the trimethoxybenzoyl group should be placed. The aromatic substituents (*m*-OCH₃-C₆H₄, *p*-F-C₆H₄, and so on) were selected from the corresponding reference (25, 26). After checking carefully, the total of D-series compounds amounted to 105. As the same with D-series in the design process, 36 E-series compounds, 72 F-series compounds, and 30 G-series compounds were prepared according to each procedure. In totally, there were 691 novel molecules generated as tubulin inhibitors.

Performance of Docking-Based and Binding Energy-based VS

There were three common docking protocols (Glide 5.8 (41), Surflex (42), and CDOCKER (16)) employed in our lab. However, comparison of molecular docking studies on in-house compounds as B-raf inhibitors using these three software above, the obtained result by CDOCKER 3.5 exhibited better than the other two docking protocols. Therefore, we artificially adopted CDOCKER protocol as main docking-based VS platform. Initially all the 692 compounds (691 designed molecules and the positive control colchicine) were docked into the reported X-ray structures of Tubulin (PDB code: 1SA0) and generated 6920 binding poses. According to the values of CDOCKER_INTERACTION_ENERGY and the possibility of gain for each binding pose, the most optimized binding conformation of each molecule had been obtained. Compared with the control molecule colchicine (Table

S2), we roughly ranked 322 molecules, of which CDOCKER_INTERATION_ENERGY ranged from -72.02 to -55.4538 kcal/mol. As expected, the docking energy of the best molecule (**D-101**) was much lower than that of the control molecule (-55.4257 kcal/mol).

On the basis of molecular docking analyses, the obtained 323 molecules (322 + colchicine) were optimized, and evaluated by the binding energy term between protein and ligands. All the calculation was performed on the Discovery Studio suite 3.5, in which the binding energy protocol was involved with two key settings: *in situ* ligand minimization and implicit solvent (43). Therefore, all the 323 molecules were firstly simulated in the setting of *in situ* ligand minimization using the CHARMM force field, and then added into poisson–boltzmann surface area (PB/SA) model for binding energy calculation. The calculated result were displayed in Table S3. Comparison of these compounds with the positive molecule colchicine, we roughly ranked 215 molecules, of which CDOCKER_INTERATION_ENERGY ranged from -167.862 to -79.2536 kcal/mol. As expected, the binding energy of the best molecule (**B-94**) was much lower than that of the control molecule (-79.2536 kcal/mol).

Performance of 3D-QSAR-Based VS

3D-QSAR model can correlate compound activities with interaction fields calculated based on protein crystallography or molecule superimposition. The success of any QSAR model depended on several factors, such as accuracy of input data, the choice of descriptors and statistical methods for modeling and for validation (44). Firstly, with regard to the input data, a total of 116 molecules (114 arylthioindoles/thiazoles/benzo[b]furan, plus the two control molecules colchicine and CA4) as potent tubulin inhibitor was collected from the continuous work of Silvestri group (19-26) and Kremmidiotis group (27). In this work, the *in vitro* biological activities of these compounds for inhibition of tubulin polymerization were converted into the corresponding pIC₅₀ (-log Ki) values (Table S4), which were used as dependent variables in the 3D-QSAR model. Due to the discrepancy of the activity measure used in different papers, we simply modified the IC₅₀ values of compounds **86-97** (25), **98-108** (27), **109-113** (26) by comparing CA4 activity values between in refs (16-21) and refs (22-24) (Table S4). In addition, it was acceptable that the activity value of these compounds ranged from 0.67 to 15 μM. The collected compounds were randomly divided into a training set (including 93 compounds) and a test set (including 23 compounds) in an approximate ratio of 4:1. Second, molecular alignment of compounds played a crucial role in the development of

3D-QSAR models (45). So far, there were two common methods used for molecular alignment of compounds (ligand-based superimposition and docking-based superimposition). Owing to structural diversity of the selected 116 compounds, we performed molecular docking study of these molecules, and then selected their optimal pose for molecular alignment, which can be clearly demonstrated in Figure 4a.

According to the 3D-QSAR procedure in the Discovery Studio suite 3.5, the corresponding model was built easily. To validate whether a QSAR model was robust for prediction of unknown molecules, three statistical parameters in DS 3.5 including especially the cross-validated correlation coefficient (q^2), correlation coefficient (r^2), and root mean square error (RMS) should be evaluated. For this 3D-QSAR studies of 116 CSIs, acceptable correlations were observed in the obtained model demonstrated by the tolerated value of q^2 (0.452) and good correlation coefficient r^2 (0.921). As shown in Figure 4b, the correlations between the experimental and the predicted activities for both the training and test sets for the optimal 3D-QSAR model. Obviously, all the points are rather uniformly distributed around the regression line, suggesting the satisfactory predictive capability of the models. The detailed values depicted by the QSAR model were list in Table S4. The 3D-QSAR result was used to be represented as 3D coefficient contour (Figure 4c and 4d). It showed regions located in the colchicine-binding pocket where variations of the steric and electrostatic nature of compounds can lead to the increase or decrease in the activity. To aid in visualization, the positive molecule colchicine was displayed superimposed with the contour maps. For example, to increase the activity of colchicine, we should add polar groups with positive electrostatic potential in the red area, and add that with negative electrostatic in the blue area. Figure 4d showed van der Waals (VDW) interactions of 3D-QSAR. Green indicates positive coefficients; violet indicates negative coefficients. In the same way, to increase activity, a new molecule should have strong VDW attraction in the green area and weak VDW attraction in the violet area. As shown in Figure 2, The activities of the 225 molecules for tubulin inhibition was predicted based on the 3D-QSAR model. Compared with the control molecule colchicine (Table S5), we roughly ranked 51 molecules. The best compound was **D-29** with the predicted pIC_{50} value of 6.07586.

Performance of Pharmacophore-Based VS

Forty-eight molecules was a large number for the result of VS. Therefore, there was a need for reducing the scope of these novel CSIs. In this section, we selected ten of the most active compounds of each literature (19-27) discussed above for generating the complex-based pharmacophore models. These molecules were compound **24**, **64**, **72**, **81**, **82**, **85**, **94**, **100**, colchicine and CA4 (Table 1). Meanwhile, we picked up 53 active molecules from the previous 116 QSAR molecules as the active set of pharmacophore establishment, and prepared 21 inactive in-house benzimidazole molecules as the inactive set (Table S2). For each complex, all the generated pharmacophore models could be ranked by the selectivity scores, and the prediction capacity of each pharmacophore model to distinguish the active inhibitors from the inactive molecules was evaluated by the **Accuracy** values. One compound could produce one optimal pharmacophore model. Finally, ten kinds of tubulin colchicine-site pharmacophore models based on various structure molecules were successfully built (Table 1, pharmacophore **a-j**). All pharmacophoric features were derived from the protein–ligand interactions. One other thing to note was that while all the models can possess several same kinds of features, their coordinates in the active pocket were different.

According to the screening steps provided in Figure 2, the 51 screened molecules were imported into these pharmacophore models mentioned above for virtual evaluation. To our disappointment, the pharmacophore **h** model built based on compound **100** could not work as the others. Therefore, Table 2 just listed the final results screened by the other nine pharmacophore models. Due to each pharmacophore model possessed different features that can reveal the structural diversity of these 51 molecules, we ranked all the results by the consensus score that combined with the fitvalues of nine pharmacophore models. Briefly, if the fitvalue of each compound was in the top 20% of one pharmacophore's evaluation system, the consensus number would automatically be added one. Thus the consensus score was a integer, and the high the value was, the better the compound performed. Analysis of the results in Table 2 showed most of compounds in front of colchicine could covered several pharmacophore models. The best molecule A-46 possessed high fitvalues in a series of pharmacophore models (pharmacophore **b-e**). In addition, chemical structures of the ultimate 16 molecules was demonstrated in Figure 6. Strikingly, the parent nucleus of these compounds come from A, B, C, D, and E-series, displaying their structural diversity.

Validation of Availability of The Design Strategy

Among the 16 designed molecules, compound **A-132** with *in silico* moderate activity was synthesized as tubulin polymerization inhibitor in this manuscript (Scheme 1). The detailed synthesis was described in the Experimental Section. Figure 7b showed the antiproliferative activities of compound **A-132** and the control molecule colchicine, and obviously compound **A-132** can be comparable to colchicine in these three cancer cell assay, particularly performing better than colchicine in the antiproliferative activities against HepG2 cells. In addition, we examined the inhibitory activity of compound **A-132** for tubulin polymerization assay, of which the IC₅₀ value could reach up to 1.64 μ M, slightly superior to that of colchicine.

Immunofluorescence assay of compound **A-132** was performed on HepG2 cells (hepatocellular carcinoma cell) by using anti-tubulin antibody and DAPI nuclear staining agent. As shown in Figure 7c, the microtubule network exhibits normal arrangement and organization in HepG2 in the absence of drug treatment (Figure 7 c1). As expected, with the increasing concentration of compound **A-132** ranging from 0.64 to 6.4 μ M after 24 h drug treatment, HepG2 cell seemed obviously to shrink in size, and cellular microtubule significantly displayed depolymerization in a concentration-dependent manner (Figure 7 c2 ~ c4). Molecular docking of compound **A-132** was performed in the tubulin active pocket (PDB code: 1SA0, Figure 8). As the same with these known CSIs mentioned in the SAR analysis section, compound **A-132** can be inserted better into the active pocket of tubulin. Although it did not contain the trimethoxybenzoyl moiety in the subpocket formed around the key residues (CYS241, LEU242, and ILE378) when compared with colchicine (Figure 8b), this molecule could make full use of the space in the binding site, particularly the modification of 3-methoxyphenyl and methyl in the C region. Additionally, the predicted binding mode of compound **A-132** was in accordance with the speculated in advance. Thus, insight into deep analysis of the binding site can contribute to the better design of CSIs.

CONCLUSION

In the present study, we manually curated a small-size CSI database composed of 691 molecules covering several heterocycle scaffolds in the field of medicinal chemistry, and subsequently performed structure-based virtual screening against colchicine binding site. In order to improve the success of hits by VS, the design process of these compounds appeared a bit conservative, of which their structure might be more close to the reported CSIs. For

making a balance between the computational cost and prediction efficiency, we employed a hierarchical strategy by integrating various computational methods in an increasing order of complexity. Besides, homogeneous distributions of the number of designed compounds from different series at each stage of VS (Figure 9) validated the reliability of this tactics or the rationality of various structure compounds. Combining molecular docking, 3D-QSAR model, and complex-based pharmacophore searching based on tubulin protein structure, sixteen novel compounds (Figure 6) with various structural features were obtained, among which compound **A-132** has been synthesized, and preliminary biological assay of **A-132** for tubulin polymerization inhibition can provide the accuracy of this kind of rational drug design. So far, the other fifteen target compounds are being synthesized in our lab, and they can be served as the starting points for the development of novel tubulin inhibitors.

METHODS AND MATERIALS

Computational Section

The SAR Analysis

All the compounds used in this study were extracted from a series of recently published literature (19-27). The compounds displayed in Chart 1 were picked up manually, and each molecule exhibited most potent activity in the corresponding paper. The protein-ligand interaction maps was depicted based on the optimal pose of this compound from the docking study. Partitions of the modification space were roughly from individual subjective judgment, and they were not exact. However, this was just to aid the SAR analysis.

Molecular Docking

Molecular docking of compounds into the three dimensional X-ray structure of human tubulin complex (PDB code: 1SA0) was carried out using the Discovery Studio (version 3.5) as implemented through the graphical user interface DS-CDOCKER protocol. The 3D structure of tubulin (1SA0) in docking study was downloaded from Protein Data Bank. The three-dimensional structures of the aforementioned compounds were constructed using Chem. 3D ultra 12.0 software [Chemical Structure Drawing Standard; Cambridge Soft corporation, USA (2010)],

then they were energetically minimized by using MMFF94 with 5000 iterations and minimum RMS gradient of 0.10. All bound waters and ligands were eliminated from the protein and the polar hydrogen was added to the proteins. Each compounds would retain 10 poses, and were ranked by CDOCKER_INTERACTION_ENERGY. The selection of the conformation of each compound would partly depend on the binding mode in the active pocket, when compared those known inhibitors, such as CA4, colchicine, and so on.

3D-QSAR

3D QSAR model provided useful information about the correlation between the molecular fields and the activity. All the operations were also performed on the the Discovery Studio suite 3.5. 116 compounds were carefully picked up from the literature mentioned above, and it needed considering the activity range of these compounds. However, their IC₅₀ values could not span 4 orders of magnitude, mainly due to the less active molecule reported in these papers had not enough and reliable data. The docking study was carried out to obtain reasonable molecular alignments for building 3D-QSAR model. In addition, the parameter for cross-validation was set to 10.

Pharmacophore Model

The complex-based pharmacophore model can be obtained directly from ligand-protein co-crystal structure that can reflect more reliable information about the structural features required for the relating biological potency in the binding site. The complex-based pharmacophore models for ten tubulin complexes selected from the corresponding docking study were generated by using the Receptor–Ligand Pharmacophore Generation (RLPG) protocol in DS3.5. Generally pharmacophoric features include hydrogen bond acceptor/donor (HBA/HBD), hydrophobic (HYD), negative/positive ionizable (PI/NI), and ring aromatic (RA) features in the DS suite. For each pharmacophore model, we provided the same set of active molecules(53 compounds selected from the QSAR study) and inactive molecules (21 in-house compounds, Chart S2) for the validation of pharmacophore models.

Experimental Section

Chemistry

The synthetic route of compound **A-132** is outlined in Scheme 1. Firstly, compound **s2** were prepared by vilsmeier reaction. Second , Compound **s3** were prepared according to the procedure reported by Debajyoti Saha *et al.* with some modifications. Compound **s4** were synthesized from compound **s3** reacting with 1-(3-methoxyphenyl) ethanone at room temperature. The mixture of compound **s4** and hydrazine hydrate in CH₃CH₂OH was refluxed under stirring for 8 h and the precipitate formed was filtered off, washed with cool ethanol to get compound **s5**. Finally, compound **s5** reacted with 3-methoxybenzoic acid, together with EDC·HCl and HOBt. The mixture was refluxed under stirring for 24 h. The crude product was crystallized with ethanol to give target compound **A-132**. Compounds **A-132** were fully characterized by ¹H NMR, ESI-MS and elemental analysis.

Chemistry general

All chemicals and reagents of analytical grade used were purchased from Aldrich (USA). Melting points (uncorrected) were determined on a XT4MP apparatus (Taik Corp, Beijing, China). All the ¹H NMR spectra were recorded on a Bruker DPX 300 model Spectrometer at 25 °C with TMS and solvent signals allotted as internal standards, and chemical shifts were reported in ppm (*d*). ESI-MS spectra were recorded on a Mariner System 5304 Mass spectrometer. Elemental analyses were performed on a CHN-O-Rapid instrument and were within 0.4% of the theoretical values. TLC was performed on the glass-backed silica gel sheets (Silica Gel 60 GF254) and visualized in UV light (254 nm). Column chromatography was performed using silica gel (200-300 mesh) eluting with ethyl acetate and petroleum ether.

5-methoxy-1H-indole-3-carbaldehyde (s2) was prepared according to the following procedure. To a solution of DMF (20 mL) was added POCl₃ (10 mL) in one portion at 0 °C, and then gradually heated up to room temperature for 2 h. A solution of 5-methoxy-1H-indole (**s1**, 3.6 g, 24.7 mmol, dissolved in 10 mL DMF) was then added to the mixture at that temperature. The mixture was further heated at 60 °C for 1 h. After cooled to room temperature, the mixture was poured into ice-water slowly and then adjusted pH to 9.0 with NaHCO₃. The precipitated cake was

collected by filtration, after rinsing and drying with water. The crude product was purified by column chromatography (1 : 2 V (EtOAc)/V (hexanes) to get compound **s2**, a light yellow powder, yield 80%.

5-methoxy-1-methyl-1H-indole-3-carbaldehyde (s3) To a suspended solution of NaH (0.60 g, 60% dispersion in mineral oil, 25 mmol) in THF (5 mL), 5-methoxy-1H-indole-3-carbaldehyde (**s2**, 1.76 g, 10 mmol) dissolved in THF (5 mL) was added dropwise at 0 °C. The heterogeneous mixture was stirred at 0 °C for 15 min and 1 h at room temperature. The mixture was then cooled to 0 °C with iodomethane (0.84 mL, 13.2 mmol), and allowed from warm to room temperature. After 30 min, the reaction mixture was cooled to 0 °C, quenched with saturated NH₄Cl (20 mL), and extracted with ether (35 mL). The organic layers were combined, washed with brine, dried over anhydrous Na₂SO₄ and concentrated *in vacuo*. The resulting oil was purified by flash column chromatography to provide 5-methoxy-1-methyl-1H-indole-3-carbaldehyde, a light yellow oil, yield 67.8%.

(E)-1-(5-methoxy-1-methyl-1H-indol-3-yl)-3-(3-methoxyphenyl) prop-2-en-1-one (s4) To a stirred solution of 1-(3-methoxyphenyl) ethanone (1 mmol) and 5-methoxy-1-methyl-1H-indole-3-carbaldehyde (**s3**, 1 mmol) in ethanol (30 mL), 6 mol KOH (4 mL) was added and the reaction mixture was stirred until the solids fully formed. The products were filtrated and washed carefully with ice water and cool ethanol, and purified by crystallization from ethanol in refrigerator to give (E)-1-(5-methoxy-1-methyl-1H-indol-3-yl)-3-(3-methoxyphenyl) prop-2-en-1-one (compound **s4**) a yellow powder, yield 60%.

5-methoxy-3-(3-(3-methoxyphenyl)-4, 5-dihydro-1H-pyrazol-5-yl)-1-methyl-1H-indole (s5) To a solution of compound **s4** (1 mmol) in isopropanol (5 mL) hydrazine hydrate (0.2 mL, 4 mmol) was added. The mixture was refluxed under stirring for 8 h, stored at 4~5 °C for 24 h, and the precipitate formed was filtered off, washed with cool ethanol. The synthesized compound was purified by crystallization from ethanol in refrigerator to give 5-methoxy-3-(3-(3-methoxyphenyl)-4, 5-dihydro-1H-pyrazol-5-yl)-1-methyl-1H-indole (**s5**), yellow powder, yield 40%.

(5-(5-methoxy-1-methyl-1H-indol-3-yl)-3-(3-methoxyphenyl)-4, 5-dihydro-1H-pyrazol-1-yl)(3-methoxyphenyl) methanone (A-132) To a solution of compound **s5** (1 mmol) in dichloromethane (5 mL) and 3-methoxybenzoic acid (1 mmol) was added, together with EDC·HCl (1.2~1.5 mmol) and HOBT (1.2~1.5 mmol). The mixture was refluxed under stirring for 24 h. After completion of the reaction, the contents were cooled, and then evaporated to dryness *in*

vacuo. Aqueous hydrochloric acid (0.1 M, 30 mL) was added and the mixture extracted with ethyl acetate (3 × 5 mL). The combined ethyl acetate layers were back-extracted with saturated sodium bicarbonate (1 × 5 mL) and brine (1 × 5 mL), dried over MgSO₄, filtered, and evaporated *in vacuo*. The residue was crystallized from ethanol to give target compound **A-132**. White crystals, yield 76.7 %. Mp: 128-130 °C. ¹H NMR (400 MHz, DMSO, δ ppm): 7.45 – 7.34 (m, 5H), 7.30 (t, *J* = 4.4 Hz, 3H), 7.12 – 7.02 (m, 2H), 6.88 (s, 1H), 6.79 (dd, *J*₁ = 8.84 Hz, *J*₂ = 8.84 Hz, 1H), 6.01 (dd, *J*₁ = 11.64 Hz, *J*₂ = 11.72 Hz, 1H), 3.88 (dd, *J*₁ = 18 Hz, *J*₂ = 17.92 Hz, 1H), 3.78 (d, *J* = 2.4 Hz, 6H), 3.71 (s, 3H), 3.58 (s, 3H), 3.31 (dd, *J*₁ = 18 Hz, *J*₂ = 17.92 Hz, 1H). MS (ESI): 470.53 [M+H]⁺; Anal. Calcd. for C₂₈H₂₇N₃O₄: C, 71.62; H, 5.80; N, 8.95; O, 13.63; Found: C, 71.63; H, 5.79; N, 8.96; O, 13.64.

Biological assay

Cell proliferation assay (Cell viability was assessed by MTT assay)

We evaluated the antiproliferativities of compounds **A-132** against A549 (carcinomic human alveolar basal epithelial cell), HepG2 (human hepatocellular carcinoma cell line), and MCF-7 (breast cancer) cancer cells with analysis. Cell proliferation was determined using the MTT dye (Beyotime Inst Biotech, China) according to the instructions of manufacture. Briefly, 5 × 10³ cells per well were seeded in a 96-well plate, grown at 37 °C for 12 h. Subsequently, cells were treated with compounds (**A-132** and Colchicine) at increasing concentrations in the presence of 10% FBS for 24 h. After 10 μL MTT dye was added to each well, cells were incubated at 37 °C for 3-4 h. Then all the solution in the wells was poured out and 150 μL DMSO was added to every well. Plates were read in a Victor-V multilabel counter (Perkin-Elmer) using the default europium detection protocol. Percent inhibition or GI₅₀ values of compounds were calculated by comparison with DMSO-treated control wells. The results are shown in Figure 7b.

Tubulin Polymerization assay

To evaluate the effect of the compounds on tubulin polymerization *in vitro*, different concentrations of the two compounds (colchicine and **A-132**) were preincubated with 10 μM bovine brain tubulin in glutamate buffer at 30 °C and then cooled to 0 °C. After addition of 0.4 mM GTP, the mixtures were transferred to 0 °C cuvettes in a recording

spectrophotometer and warmed to 30 °C. Tubulin assembly was followed turbidimetrically at 350 nm. The IC₅₀ was defined as the compound concentration that inhibited the extent of polymerization by 50% after 20 min incubation.

Immunocytochemistry

HepG2 cell line plated on coverslips was treated with indicated concentration of test agents for the selected treatment duration. After treatment, Cells were washed twice in PBS and fixed in 2% paraformaldehyde for 20 min at room temperature. Cells were permeabilized in PBS with 0.1% Na-Citrate, 0.1% TritonX-100 at room temperature for 15 min. Nonspecific binding sites were blocked by incubating the cells in 5% BSA. Cells were then incubated with tubulin antibody (Beyotime, AT108, China) followed by conjugated secondary IgGs (Beyotime, A0539, China) and DAPI (1 µg/ml). After incubation, cells were washed with PBS. Cellular microtubules were observed with an Olympus BX50 fluorescence microscope.

Figure/Table/Chart/Scheme Captions

Figure 1 Chemical structures of CSIs in clinical trials currently.

Figure 2 Flowchart of the whole structure-based hierarchical virtual screening strategy.

Figure 3 Design protocol based on different scaffolds. The A, B, C, and D region represented the modified space in the active pocket of tubulin.

Figure 4 3D-QSAR model. a) The molecular alignment of 116 compounds in the data set based on the docking study; b) Predicted versus actual pIC₅₀ for the 3D-QSAR model. The training set was marked in black dot and test set marked in red asterisk; c) 3D-QSAR electrostatic contour plots with the combination of colchicine. Red contours indicate regions where negative charges increase activity, and blue contours indicate regions where positive charges increase activity. d) 3D-QSAR steric contour map with the combination of colchicine. Green contours indicate regions where bulky groups increase activity, and violet contours indicate regions where bulky groups decrease activity.

Figure 5 Ten complex-based pharmacophore models developed for virtual screening (VS). green: hydrogen-bonding acceptor; pink: hydrogen-bonding donor; cyan: Hydrophobic; grey: excluded volume.

Figure 6 Chemical structures of the ultimate sixteen novel compounds.

Figure 7 a) Chemical structures of compound **A-132**; b) In Vitro inhibition of tubulin polymerization, growth of three common cancer cells (A549, HepG2, and MCF-7) by compound

A-132 and colchicine; c) Immunofluorescence microscopy detection in HepG2 cells; tubulin (red) and DAPI nuclear staining (blue); cells were treated for 24 h with compound **A-132** (**c2~c4**).

Figure 8 a) Focused view of predicted binding model of compound **A-132** (green, stick) in context of surrounding residues (cyan, stick); b) Focused view of predicted binding model of colchicine (green, stick) in context of surrounding residues (cyan, stick).

Figure 9 Distributions of the number of designed compounds belonged to different series for each stage of virtual screening (VS).

Table 1 Numbers of total features, selectivity score, and accuracy of the pharmacophore models based on ten potent tubulin inhibitors.

Table 2 The screening results obtained by using the pharmacophore models based on nine active tubulin inhibitors.

Scheme 1. Synthesis of compounds **A-132**. Reagents and conditions: (i) DMF, POCl₃; (ii) NaH, CH₃I, THF; (iii) EtOH, NaOH, r.t.; (vi) NH₂·NH₂·H₂O, EtOH, reflux; (v) EDC·HCl, HOBT, Cl₂H₂, reflux.

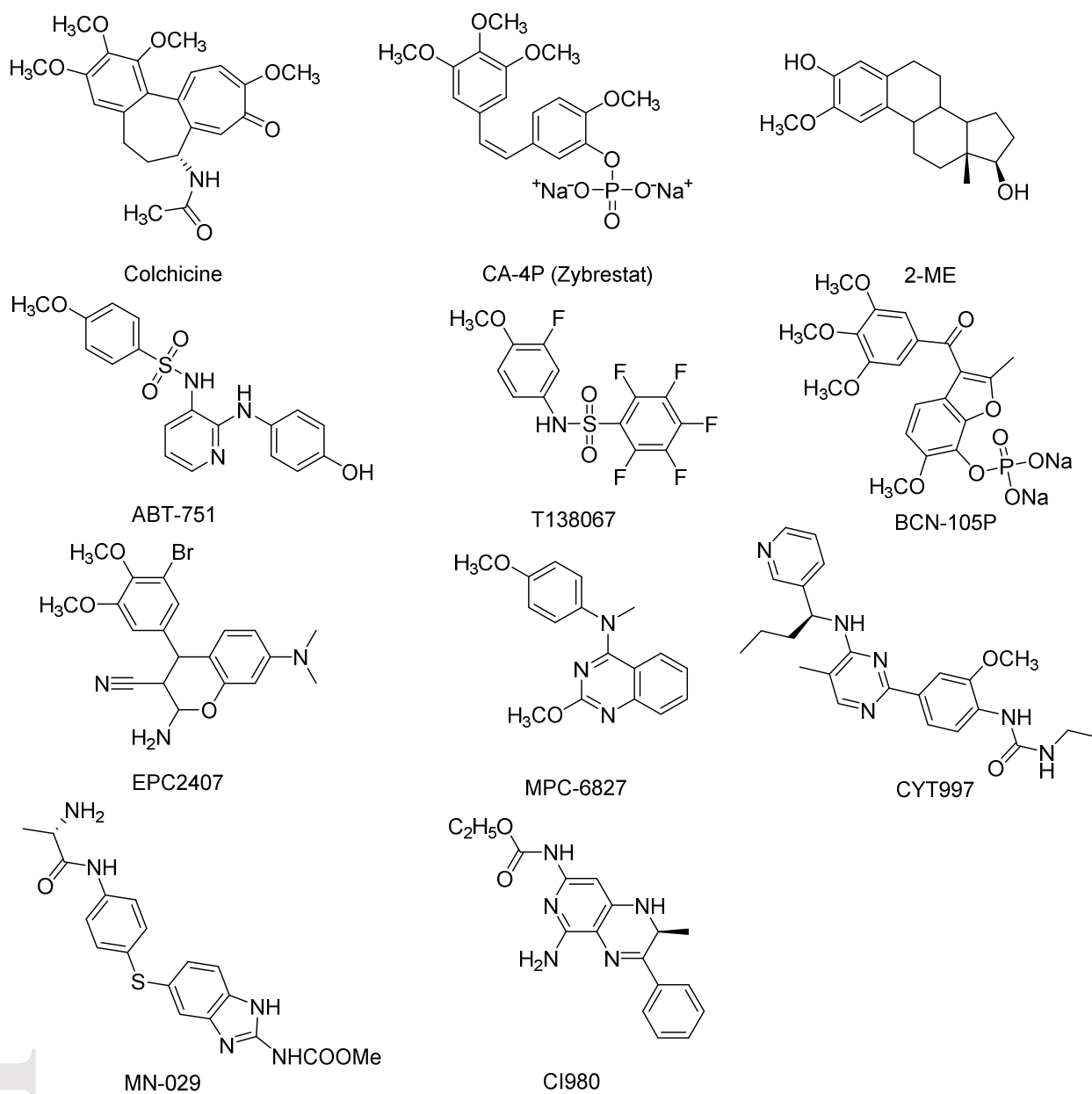


Figure 1 Chemical structures of CSIs in clinical trials currently.

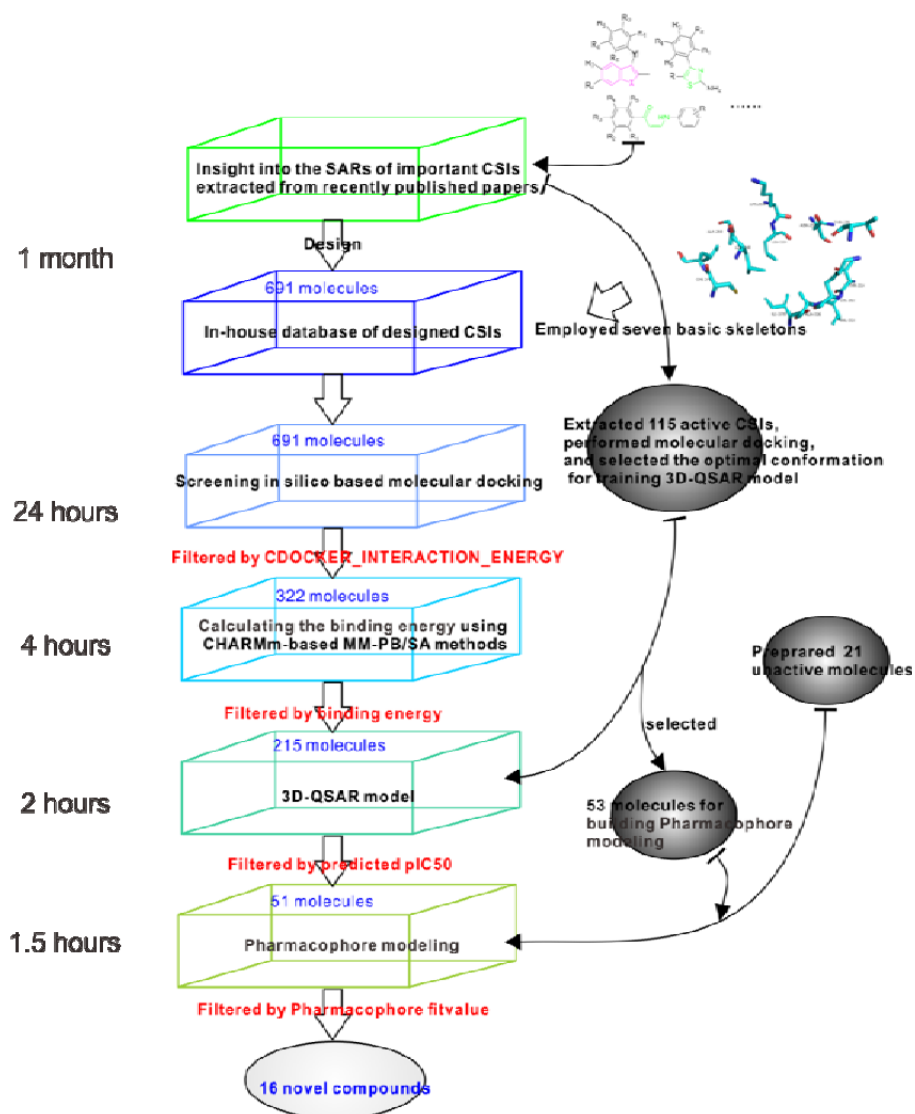


Figure 2 Flowchart of the whole structure-based hierarchical virtual screening strategy.

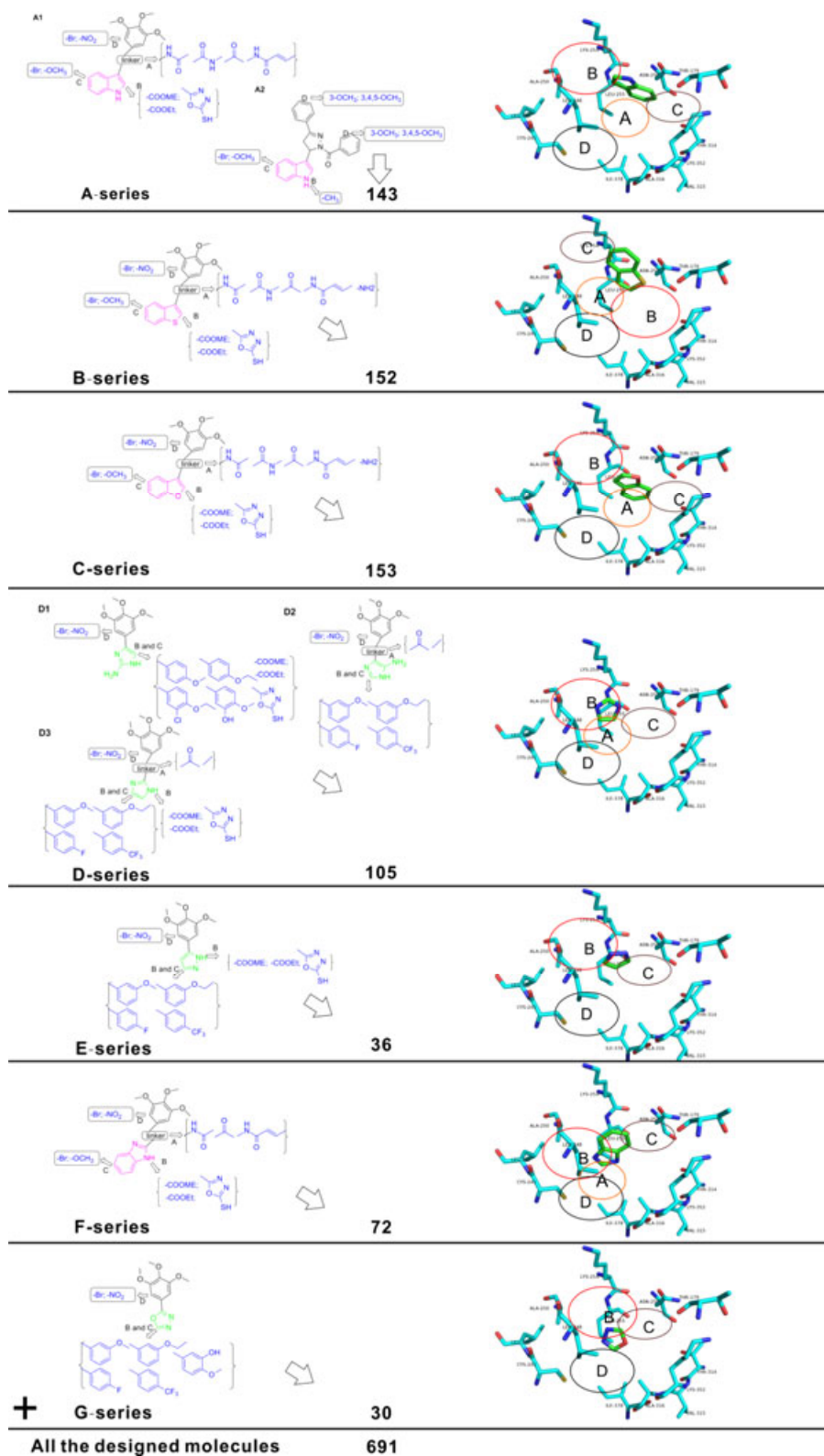


Figure 3 Design protocol based on different scaffolds. The A, B, C, and D region represented the modified space in the active pocket of tubulin.

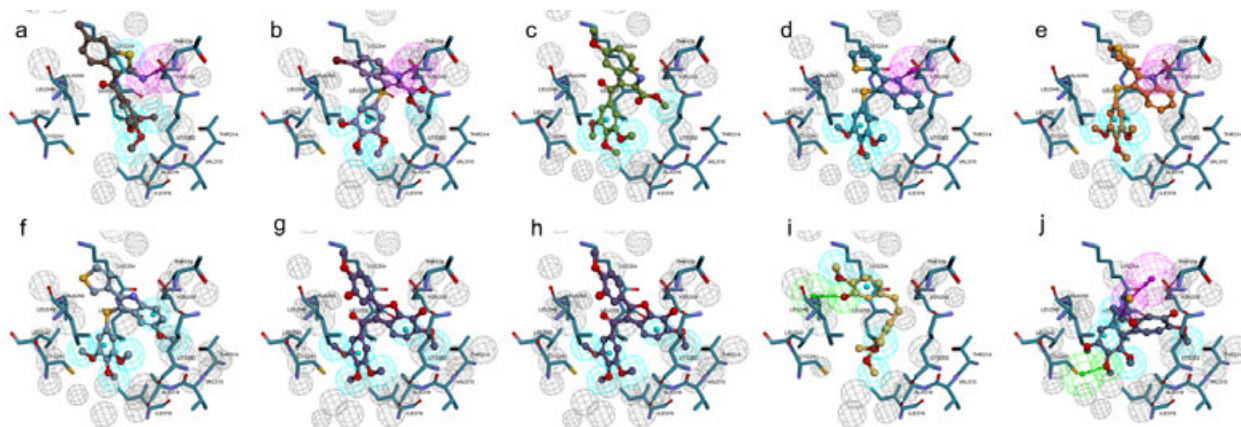


Figure 5 Ten complex-based pharmacophore models developed for virtual screening (VS). green: hydrogen-bonding acceptor; pink: hydrogen-bonding donor; cyan: Hydrophobic; grey: excluded volume.

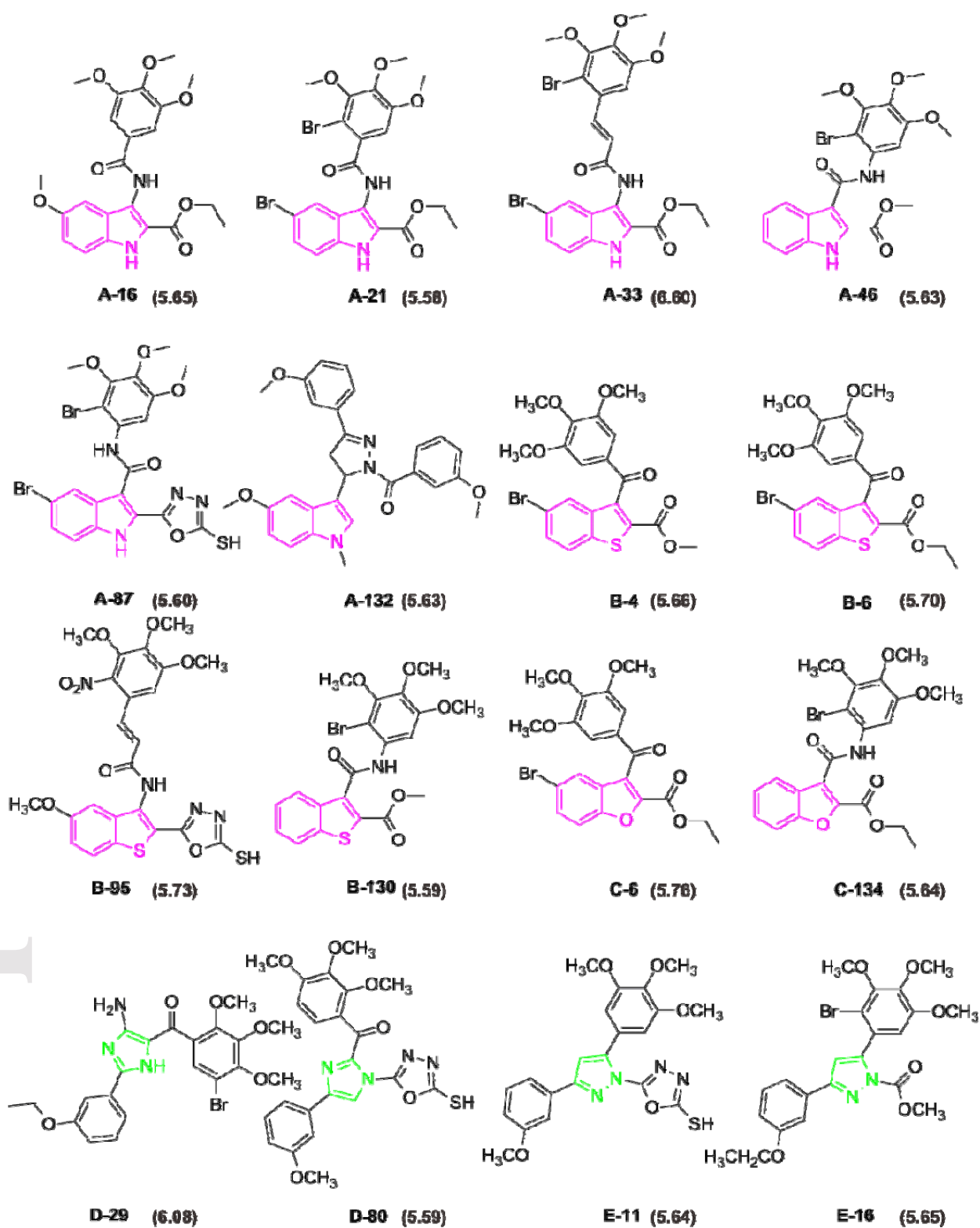


Figure 6 Chemical structures of the ultimate sixteen novel compounds and the corresponding predicted IC_{50} values against tubulin assembly.

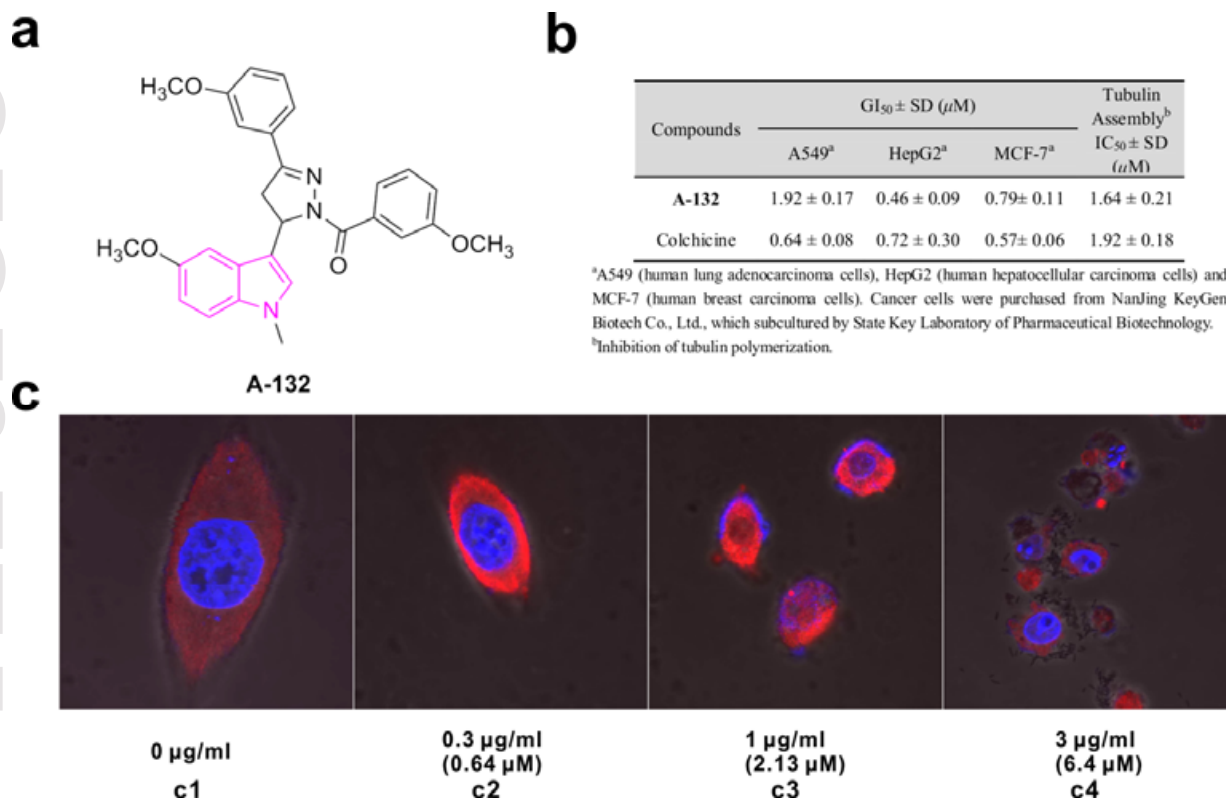


Figure 7 a) Chemical structures of compound **A-132**; b) In Vitro inhibition of tubulin polymerization, growth of three common cancer cells (A549, HepG2, and MCF-7) by compound **A-132** and colchicine; c) Immunofluorescence microscopy detection in HepG2 cells; tubulin (red) and DAPI nuclear staining (blue); cells were treated for 24 h with compound **A-132** (**c2~c4**).

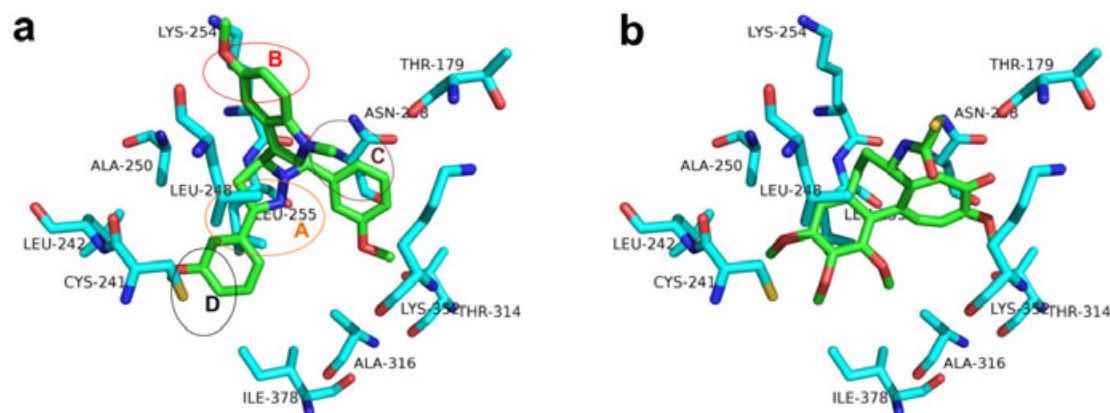


Figure 8 a) Focused view of predicted binding model of compound **A-132** (green, stick) in context of surrounding residues (cyan, stick); b) Focused view of predicted binding model of colchicine (green, stick) in context of surrounding residues (cyan, stick).

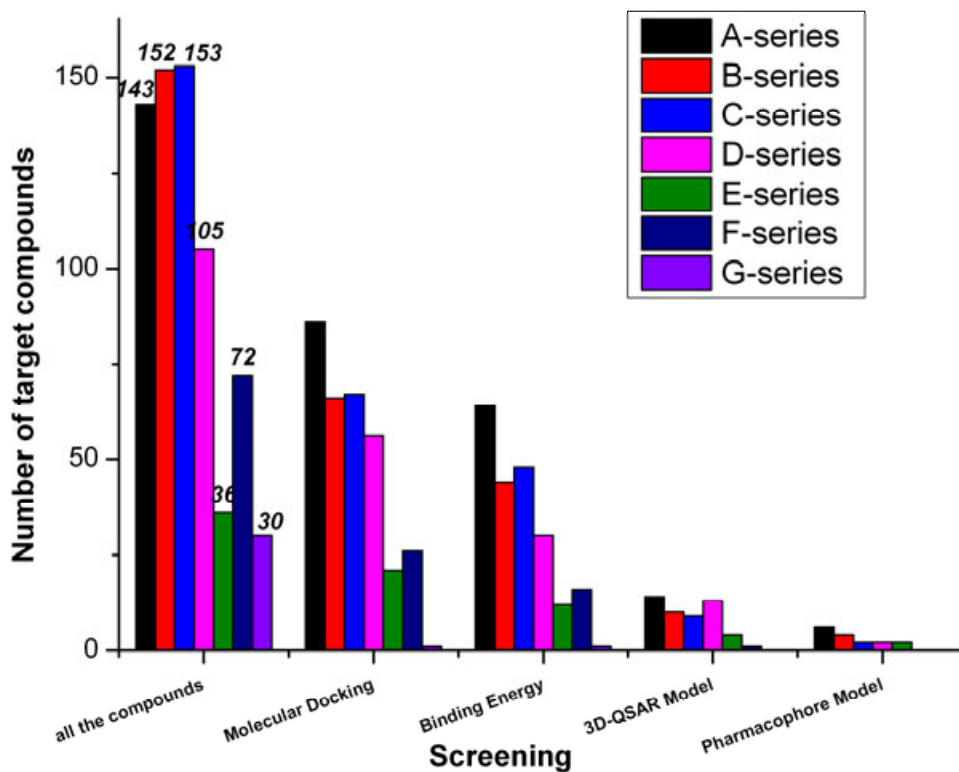
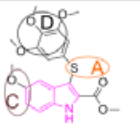
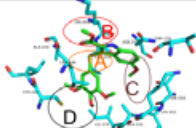
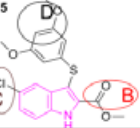
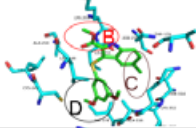
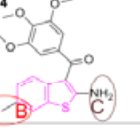
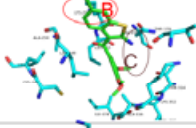
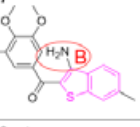
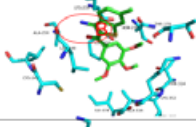
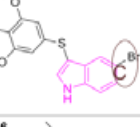
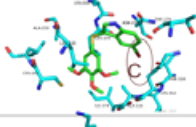
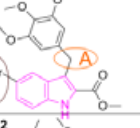
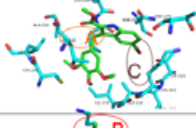
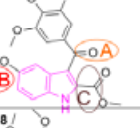
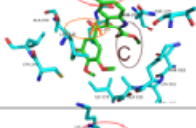
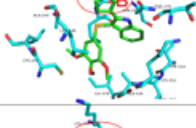
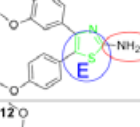
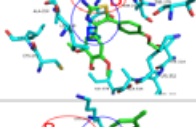
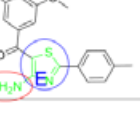
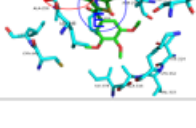


Figure 9 Distributions of the number of designed compounds belonged to different series for each stage of virtual screening (VS).

Chart 1. Analysis of structure-activity relationship (SAR) for potent tubulin inhibitors
 extracted from recently published papers.

The Optimized Lead Compounds	Protein-Ligand Interaction Maps	Structure-Activity Relationship (SAR)	Year	Reference
		A: Sulfide oxidation state reduced potency; B: Methoxy/Ethoxycarbonyl group increase potency; C: Methoxy group enhance potency; D: 3,4,5-trimethoxyphenyl moiety important.	2004	19
		B: Large alkoxy chains reduces potency; C: Electron-donating group enhance potency; the methoxy group on the indole position 4 or 6 leads to loss of activity; D: Methoxy group located para can largely influence activity.	2006	20
		B: 6-Methyl group plays a vital role in antiproliferative activity potency; C: 2-Amino substituent enhances potency.	2007	21
		B: 3-Amino substituent might be important in restricting the conformation of the adjacent trimethoxybenzoyl moiety through an intramolecular hydrogen bond with the carbonyl oxygen.	2007	21
		C: Compounds bearing a halogen atom or a small alkyl or ether group at position 5 of the indole, were also potent inhibitors of MCF-7 cell growth.	2007	22
		A: The methylene moiety is acceptable; C: Either a bromine atom or a methoxy group at position 5 and the 2-methoxy-carbonyl group at position 2 of the indole ring can increase inhibition of tubulin assembly.	2009	23
		A: The ketones moiety is reasonable; B and C: Both methoxy group at position 5 and the 2-methoxy-carbonyl group at position 2 of the indole ring can increase inhibition of tubulin assembly.	2009	23
		B: More active in the Pgp-overexpressing NCI/ADR-RES cell line; shows selective activity against cells with acquired cisplatin resistance; possesses a low systemic clearance and excellent oral bioavailability.	2011	24
		B: 2-Amino substituent enhances potency; E: Replacement of the indole ring with differently substituted pyrrole, imidazole, and thiazole analogues led to less clear results.	2011	25
		B: 4-Amino substituent enhances potency; E: Replacement of the indole ring with differently substituted pyrrole, imidazole, and thiazole analogues led to less clear results.	2012	26

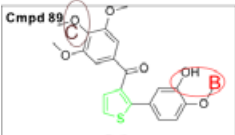
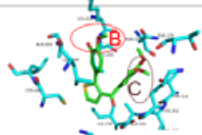
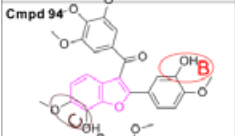
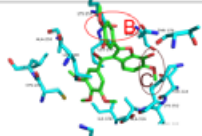
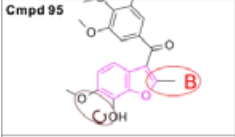
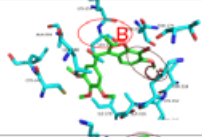
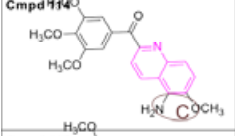
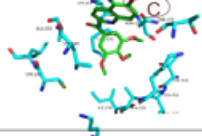
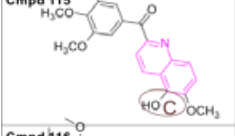
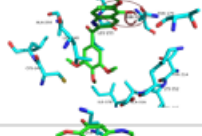
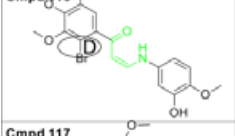
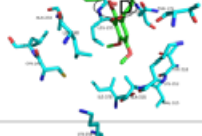
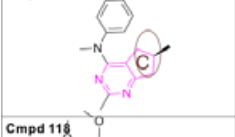
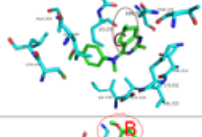
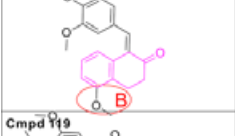
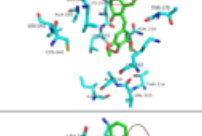
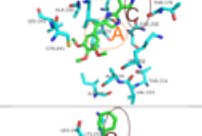
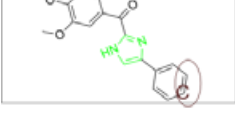
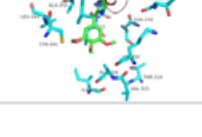
<p>Cmpd 89</p> 		<p>B and C : It is proposed that Removal of benzene linked to thiophene ring might lead to alteration of the binding conformation with tubulin protein.</p>	2011	27
<p>Cmpd 94</p> 		<p>B : While the 2-benzene ring is tolerated , it does not contribute to the potency; it could not influence the binding conformation; C : C6-methoxy is required for the potency, and C7-O H is not certified.</p>	2011	27
<p>Cmpd 95</p> 		<p>B : Both hydrophobic and hydrophilic substituents are well tolerated in the C2-position ;only the C2-methyl showed any significant selectivity; C : C6-methoxy is required for the potency, and C7-OH is not certified.</p>	2011	27
<p>Cmpd 114</p> 		<p>C : The addition of a methoxy group at the C-6 or C-8 position of the quinoline ring increased potency; trimethoxybenzoyl moiety located at the position 2 and 6 on the quinoline ring significantly contributes more in activity</p>	2010	28
<p>Cmpd 115</p> 		<p>C : C-5 hydroxy group can lead to the equivalent effect of C-5 amino group.</p>	2011	29
<p>Cmpd 116</p> 		<p>D : The inclusion of a halo or a nitro group at the ortho position moderately improved the activity of the molecules compared to the corresponding ortho-unsubstituted compound.</p>	2012	30
<p>Cmpd 117</p> 		<p>C : This modification could circumvent tumor resistance because of overexpression of Pgp and βIII tubulin</p>	2011	31
<p>Cmpd 118</p> 		<p>B : The methoxy at C-6 position buried deeper in the pocket than C-5 or C-7 position when binding, leading to the compounds bearing this group have relatively higher binding abilities</p>	2012	32
<p>Cmpd 119</p> 		<p>A : The ketone linker remained critical; C : Dimethylated 3-indole showed very good potency, indicating that a smaller group on either the imidazole- or indole-NH was well tolerated.</p>	2012	33
<p>Cmpd 120</p> 		<p>C : Introduction of an electron donating group such as methyl to the compound maintained the activity.</p>	2013	34

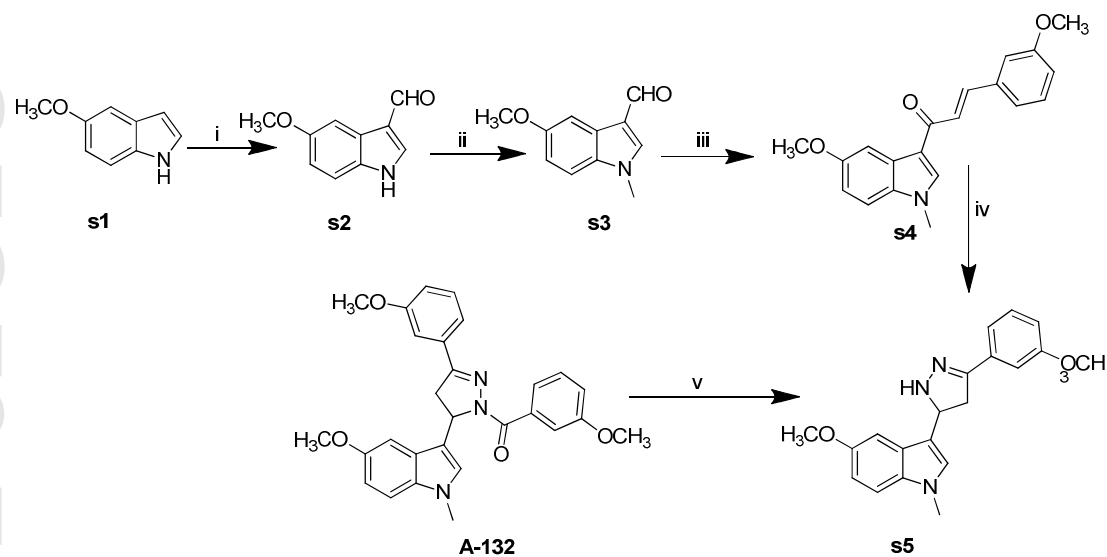
Table 1 Numbers of total features, selectivity score, and accuracy of the pharmacophore models based on ten potent tubulin inhibitors.

Pharmacophore	Pharmacophore Summary			
	Based-Ligand	Total features	selectivity score	Accuracy
Pharmacophore_a	Compound 24	DHHHH	2.1117	0.768
Pharmacophore_b	Compound 64	DHHHHH	3.3300	0.989
Pharmacophore_c	Compound 72	HHHHH	1.4740	0.897
Pharmacophore_d	Compound 81	DHHHH	2.1117	0.966
Pharmacophore_e	Compound 82	DHHHH	2.1117	0.934
Pharmacophore_f	Compound 85	HHHHHH	2.6924	0.932
Pharmacophore_g	Compound 94	HHHHHH	2.6924	0.965
Pharmacophore_h	Compound 100	DHHHH	2.1117	0.841
Pharmacophore_i	Colchicine	ADHHHH	4.5151	0.945
Pharmacophore_j	CA4	AHHHH	1.4740	0.866

Table 2 The screening results obtained by using the pharmacophore models based on nine active tubulin inhibitors.

Cmpd	Nine Protein–Ligand-Based Pharmacophores									Conse nsus
	Pharm ac a	Pharm ac b	Pharm ac c	Pharm ac d	Pharma c e	Pharm ac f	Phar mac g	Phar mac i	Pharma c j	
A-46	0	0.460 185	0.633 174	0.410 312	0.5076 99	0	0	0	0.0929 131	9
A-16	0	0.455 62	0	0.809 552	0.0002 62533	0	0	0	0.0693 767	7
A-87	0	0	0	0.333	0.4010	0	0	0	0	7

				127	92					
B-4	0	0	0.375 846	0	0	0.922 582	0.585 478	0	0.5525 1	7
C-6	0	0	0.816 155	0	0	0.055 1115	0.625 441	0	0.4150 79	7
E-11	0	0	0	0.162 055	0.0153 272	0	0	0	0	7
A-21	0	0.022 9212	0.131 921	0	0.0141 2	0	0	0	0	6
A-33	0	0	0.039 0253	0.112 053	0.0001 17043	0	0	0	0	6
B-130	0	0	0.605 074	0	0	0	0	0	0.0008 70695	6
B-6	0	0	0	0	0	0	0	0	0.0241 505	6
B-95	0	0	0	0	0	0	0	0	0.2762 66	6
C-134	0	0	0.761 157	0	0	0	0	0	0	6
D-29	0.0013 3543	0	0	0.035 2673	0.0213 799	0	0	0	0	6
A-132	0	0	0.428 361	0.032 1092	0	0	0	0	0.0012 891	6
D-80	0	0	0	0	0.5825 03	0	0	0	0	6
E-16	0	0	0.326 473	0	0	0	0	0	0	6
Colchi cine	0	0.042 6253	0.086 2241	0.626 284	0	0	0	0.682 723	0	6



Scheme 1. Synthesis of compounds **A-132**. Reagents and conditions: (i) DMF, POCl₃; (ii) NaH, CH₃I, THF; (iii) EtOH, NaOH, r.t.; (vi) NH₂·NH₂·H₂O, EtOH, reflux; (v) EDC·HCl, HOBT, Cl₂H₂, reflux.

ASSOCIATED CONTENT

Electronic supplementary material. Chart S1 displayed Chemical structure of designed molecules and Chart S2 listed the active and inactive selected for pharmacophore model. Table S1 listed several tubulin crystal complex; Table S2, S3, and S5 depicted a series of screening results for these targeted molecules; Table S3 depicted the training and test set for 3D-QSAR; Figure S1 showed the seven basic scaffolds employed for designing 691 molecules; Figure S2 showed the chemical structures of compounds used for 3D-QSAR. Figure S3 showed the ¹H NMR spectrum of compound **A-132**. This material is available to authorized users.

Funding Sources

Control and Rectification of Water Body Pollution (2011ZX07204-001-004)

ACKNOWLEDGMENT

This work was supported by Major Projects on Control and Rectification of Water Body Pollution (2011ZX07204-001-004), and by Henan Educational Committee (14B150036)

ABBREVIATIONS

CSIs, colchicine site inhibitors; VDA, vascular disrupting agent; VS, virtual screening; QSAR, quantitative structure-activity relationship; SAR, structure-activity relationship; Pharmac, pharmacophore.

REFERENCES

1. Jordan M.A., Wilson L. (2004) Microtubules as a target for anticancer drugs. *Nat Rev Cancer* 4: 253-65.
2. Dumontet C., Jordan M.A. (2010) Microtubule-binding agents: a dynamic field of cancer therapeutics. *Nat Rev Drug Discov* 9: 790-803.
3. Lu Y., Chen J., Xiao M., Li W., Miller D.D. (2012) An overview of tubulin inhibitors that interact with the colchicine binding site. *Pharm Res* 29: 2943-71.
4. Rustin G.J., Shreeves G., Nathan P.D., Gaya A., Ganesan T.S., Wang D., et al. (2010) A Phase Ib trial of CA4P (combretastatin A-4 phosphate), carboplatin, and paclitaxel in patients with advanced cancer. *Br J Cancer* 102: 1355-60.
5. Cao R., Liu M., Yin M., Liu Q., Wang Y., Huang N. (2012) Discovery of novel tubulin inhibitors via structure-based hierarchical virtual screening. *J Chem Inf Model* 52: 2730-40.
6. Chen S.M., Meng L.H., Ding J. (2010) New microtubule-inhibiting anticancer agents. *Expert Opin Investig Drugs* 19: 329-43.
7. Stengel C., Newman S.P., Leese M.P., Potter B.V., Reed M.J., Purohit A. (2010) Class III beta-tubulin expression and in vitro resistance to microtubule targeting agents. *Br J Cancer* 102: 316-24.
8. Ravelli R.B., Gigant B., Curmi P.A., Jourdain I., Lachkar S., Sobel A., et al. (2004) Insight into tubulin regulation from a complex with colchicine and a stathmin-like domain. *Nature* 428: 198-202.

9. Dorleans A., Gigant B., Ravelli R.B., Mailliet P., Mikol V., Knossow M. (2009) Variations in the colchicine-binding domain provide insight into the structural switch of tubulin. *Proc Natl Acad Sci U S A* 106: 13775-9.
10. Barbier P., Dorleans A., Devred F., Sanz L., Allegro D., Alfonso C., et al. (2010) Stathmin and interfacial microtubule inhibitors recognize a naturally curved conformation of tubulin dimers. *J Biol Chem* 285: 31672-81.
11. Chakraborti S., Chakravarty D., Gupta S., Chatterji B.P., Dhar G., Poddar A., et al. (2012) Discrimination of ligands with different flexibilities resulting from the plasticity of the binding site in tubulin. *Biochemistry* 51: 7138-48.
12. Bai R., Covell D.G., Pei X.F., Ewell J.B., Nguyen N.Y., Brossi A., et al. (2000) Mapping the binding site of colchicinoids on beta -tubulin. 2-Chloroacetyl-2-demethylthiocolchicine covalently reacts predominantly with cysteine 239 and secondarily with cysteine 354. *J Biol Chem* 275: 40443-52.
13. Nguyen T.L., McGrath C., Hermone A.R., Burnett J.C., Zaharevitz D.W., Day B.W., et al. (2005) A common pharmacophore for a diverse set of colchicine site inhibitors using a structure-based approach. *J Med Chem* 48: 6107-16.
14. Ducki S., Mackenzie G., Lawrence N.J., Snyder J.P. (2005) Quantitative structure-activity relationship (5D-QSAR) study of combretastatin-like analogues as inhibitors of tubulin assembly. *J Med Chem* 48: 457-65.
15. Da C., Mooberry S.L., Gupton J.T., Kellogg G.E. (2013) How to deal with low-resolution target structures: using SAR, ensemble docking, hydrophobic analysis, and 3D-QSAR to definitively map the alphabeta-tubulin colchicine site. *J Med Chem* 56: 7382-95.
16. Wu G., Robertson D.H., Brooks C.L., 3rd, Vieth M. (2003) Detailed analysis of grid-based molecular docking: A case study of CDOCKER-A CHARMM-based MD docking algorithm. *J Comput Chem* 24: 1549-62.
17. Tsui V., Case D.A. (2000) Theory and applications of the generalized Born solvation model in macromolecular simulations. *Biopolymers* 56: 275-91.
18. Accelrys Software Inc., Discovery Studio Modeling Environment, Release 3.5, San Diego: Accelrys Software Inc., 2012.
19. De Martino G., La Regina G., Coluccia A., Edler M.C., Barbera M.C., Brancale A., et al. (2004) Arylthioindoles, potent inhibitors of tubulin polymerization. *J Med Chem* 47: 6120-3.
20. De Martino G., Edler M.C., La Regina G., Coluccia A., Barbera M.C., Barrow D., et al. (2006) New arylthioindoles: potent inhibitors of tubulin polymerization. 2. Structure-activity relationships and molecular modeling studies. *J Med Chem* 49: 947-54.
21. Romagnoli R., Baraldi P.G., Carrion M.D., Lopez Cara C., Preti D., Fruttarolo F., et al. (2007) Synthesis and biological evaluation of 2- and 3-aminobenzo[b]thiophene derivatives as antimitotic agents and inhibitors of tubulin polymerization. *J Med Chem* 50: 2273-7.

22. La Regina G., Edler M.C., Brancale A., Kandil S., Coluccia A., Piscitelli F., et al. (2007) Arylthioindole inhibitors of tubulin polymerization. 3. Biological evaluation, structure-activity relationships and molecular modeling studies. *J Med Chem* 50: 2865-74.
23. La Regina G., Sarkar T., Bai R., Edler M.C., Saletti R., Coluccia A., et al. (2009) New arylthioindoles and related bioisosteres at the sulfur bridging group. 4. Synthesis, tubulin polymerization, cell growth inhibition, and molecular modeling studies. *J Med Chem* 52: 7512-27.
24. La Regina G., Bai R., Rensen W., Coluccia A., Piscitelli F., Gatti V., et al. (2011) Design and synthesis of 2-heterocyclyl-3-arylthio-1H-indoles as potent tubulin polymerization and cell growth inhibitors with improved metabolic stability. *J Med Chem* 54: 8394-406.
25. Romagnoli R., Baraldi P.G., Brancale A., Ricci A., Hamel E., Bortolozzi R., et al. (2011) Convergent synthesis and biological evaluation of 2-amino-4-(3',4',5'-trimethoxyphenyl)-5-aryl thiazoles as microtubule targeting agents. *J Med Chem* 54: 5144-53.
26. Romagnoli R., Baraldi P.G., Salvador M.K., Preti D., Aghazadeh Tabrizi M., Brancale A., et al. (2012) Discovery and optimization of a series of 2-aryl-4-amino-5-(3',4',5'-trimethoxybenzoyl)thiazoles as novel anticancer agents. *J Med Chem* 55: 5433-45.
27. Flynn B.L., Gill G.S., Grobelny D.W., Chaplin J.H., Paul D., Leske A.F., et al. (2011) Discovery of 7-Hydroxy-6-methoxy-2-methyl-3-(3,4,5-trimethoxybenzoyl)benzo[b]furan (BNC105), a Tubulin Polymerization Inhibitor with Potent Antiproliferative and Tumor Vascular Disrupting Properties. *Journal of Medicinal Chemistry* 54: 6014-27.
28. Nien C.Y., Chen Y.C., Kuo C.C., Hsieh H.P., Chang C.Y., Wu J.S., et al. (2010) 5-Amino-2-arylquinolines as highly potent tubulin polymerization inhibitors. *J Med Chem* 53: 2309-13.
29. Lee H.Y., Chang J.Y., Nien C.Y., Kuo C.C., Shih K.H., Wu C.H., et al. (2011) 5-Amino-2-arylquinolines as highly potent tubulin polymerization inhibitors. Part 2. The impact of bridging groups at position C-2. *J Med Chem* 54: 8517-25.
30. Reddy M.V., Akula B., Cosenza S.C., Lee C.M., Mallireddigari M.R., Pallela V.R., et al. (2012) (Z)-1-aryl-3-arylamino-2-propen-1-ones, highly active stimulators of tubulin polymerization: synthesis, structure-activity relationship (SAR), tubulin polymerization, and cell growth inhibition studies. *J Med Chem* 55: 5174-87.
31. Gangjee A., Zhao Y., Hamel E., Westbrook C., Mooberry S.L. (2011) Synthesis and biological activities of (R)- and (S)-N-(4-Methoxyphenyl)-N,2,6-trimethyl-6,7-dihydro-5H-cyclopenta[d]pyrimidin-4-a minium chloride as potent cytotoxic antitubulin agents. *J Med Chem* 54: 6151-5.
32. Liu J., Zheng C.H., Ren X.H., Zhou F., Li W., Zhu J., et al. (2012) Synthesis and biological evaluation of 1-benzylidene-3,4-dihydronaphthalen-2-one as a new class of microtubule-targeting agents. *J Med Chem* 55: 5720-33.

33. Chen J., Ahn S., Wang J., Lu Y., Dalton J.T., Miller D.D., et al. (2012) Discovery of Novel 2-Aryl-4-benzoyl-imidazole (ABI-III) Analogues Targeting Tubulin Polymerization As Antiproliferative Agents. *J Med Chem* 55: 7285-9.
34. Xiao M., Ahn S., Wang J., Chen J., Miller D.D., Dalton J.T., et al. (2013) Discovery of 4-Aryl-2-benzoyl-imidazoles as Tubulin Polymerization Inhibitor with Potent Antiproliferative Properties. *J Med Chem* 56: 3318-29
35. Liu X.H., Ruan B.F., Li J., Chen F.H., Song B.A., Zhu H.L., et al. (2011) Synthesis and biological activity of chiral dihydropyrazole: potential lead for drug design. *Mini Rev Med Chem* 11: 771-821.
36. Liu X.H., Ruan B.F., Liu J.X., Song B.A., Jing L.H., Li J., et al. (2011) Design and synthesis of N-phenylacetyl (sulfonyl) 4,5-dihydropyrazole derivatives as potential antitumor agents. *Bioorg Med Chem Lett*;21: 2916-20.
37. Liu X.H., Liu H.F., Chen J., Yang Y., Song B.A., Bai L.S., et al. (2010) Synthesis and molecular docking study of novel coumarin derivatives containing 4,5-dihydropyrazole moiety as potential antitumor agents. *Bioorg Med Chem Lett* 20: 5705-8.
38. Sun J., Cao N., Zhang X.M., Yang Y.S., Zhang Y.B., Wang X.M., et al. (2011) Oxadiazole derivatives containing 1,4-benzodioxan as potential immunosuppressive agents against RAW264.7 cells. *Bioorg Med Chem* 19: 4895-902.
39. Zhang X.M., Qiu M., Sun J., Zhang Y.B., Yang Y.S., Wang X.L., et al. (2011) Synthesis, biological evaluation, and molecular docking studies of 1,3,4-oxadiazole derivatives possessing 1,4-benzodioxan moiety as potential anticancer agents. *Bioorg Med Chem* 19: 6518-24.
40. Zheng Q.Z., Zhang X.M., Xu Y., Cheng K., Jiao Q.C., Zhu H.L. (2010) Synthesis, biological evaluation, and molecular docking studies of 2-chloropyridine derivatives possessing 1,3,4-oxadiazole moiety as potential antitumor agents. *Bioorg Med Chem* 18: 7836-41.
41. Friesner R.A., Banks J.L., Murphy R.B., Halgren T.A., Klicic J.J., Mainz D.T., et al. (2004) Glide: a new approach for rapid, accurate docking and scoring. 1. Method and assessment of docking accuracy. *J Med Chem* 47: 1739-49.
42. Jain A.N. (2003) Surflex: fully automatic flexible molecular docking using a molecular similarity-based search engine. *J Med Chem* 46: 499-511.
43. Tirado-Rives J., Jorgensen W.L. (2006) Contribution of conformer focusing to the uncertainty in predicting free energies for protein-ligand binding. *J Med Chem* 49: 5880-4.
44. Tropsha A., Gramatica P., Gombar V.K. (2003) The Importance of Being Earnest: Validation is the Absolute Essential for Successful Application and Interpretation of QSPR Models. *Qsar Comb Sci* 22:69-77.
45. AbdulHameed M.D., Hamza A., Liu J., Zhan C.G. (2008) Combined 3D-QSAR modeling and molecular docking study on indolinone derivatives as inhibitors of 3-phosphoinositide-dependent protein kinase-1. *J Chem Inf Model* 48: 1760-72.